

# Reduction of intersymbol interference in dispersion-managed soliton systems compensated by chirped fibre gratings using nonlinear optical loop mirrors

Y H C Kwan<sup>1</sup>, K Nakkeeran<sup>1,3</sup>, P K A Wai<sup>1</sup> and P Tchofo Dinda<sup>2</sup>

<sup>1</sup> Photonics Research Center and Department of Electronic and Information Engineering, The Hong Kong Polytechnic University, Hong Kong

<sup>2</sup> Laboratoire de Physique de l'Université de Bourgogne, BP 47 870, 21078 Dijon, France

Received 19 December 2004, accepted for publication 29 April 2005

Published 21 June 2005

Online at [stacks.iop.org/JOptA/7/315](http://stacks.iop.org/JOptA/7/315)

## Abstract

We address the problem of group delay ripples in chirped fibre gratings on dispersion compensation in optical transmission systems. We show that the intersymbol interference, which is a highly harmful effect induced by the group delay ripples in transmission systems, can be substantially reduced by the use of nonlinear optical loop mirrors. This leads to an improvement of the system performance by more than one order of magnitude when compared with a grating-compensated dispersion-managed system without nonlinear optical loop mirrors. We find similar performances irrespective of whether the structure of group delay ripples is modelled by a sinusoidal function or the grating is modelled by the coupled-mode equations.

**Keywords:** optical communications, dispersion-managed systems, gratings, group delay ripples, nonlinear optical loop mirrors

## 1. Introduction

In optical fibre communications, the most efficient technique to minimize the effect of the fibre chromatic dispersion is the technique of *dispersion management*. Now, many terrestrial transmission systems have already been installed in the field and the cost of upgrading such systems to dispersion-managed (DM) soliton systems is quite expensive. One of the most economic and easiest way to upgrade those systems is to insert lumped dispersion compensators at the amplification sites. Among the dispersion compensating methods that have appeared so far in the literature, the use of chirped fibre gratings (CFGs) appears as one of the most attractive methods because of its compact size, large lumped dispersion, low insertion loss, and zero nonlinear effects. Furthermore, CFGs, which can also compensate for higher order dispersion [1], are becoming a key issue in high-speed wavelength division multiplexed optical transmission

systems. Furthermore, it has been shown that solitons exist in DM optical fibre communication systems compensated by CFGs [2–4]. Yamada *et al* demonstrated a transmission over 2900 km for return-to-zero (RZ) formatted signals utilizing CFGs as a dispersion compensator at 10 Gb/s [5].

However, CFGs have the group delay ripples (GDR) which are caused by the imperfections in the grating fabrication process [6]. The GDR introduces side peaks in the pulse profile as illustrated in figure 1. The side peaks of each pulse overlap with the neighbouring bit slots, thus causing an intersymbol interference (ISI) which is highly detrimental to the transmission performance. In particular, in linear non-return-to-zero (NRZ) encoded transmission systems, the energy in the central peak of a pulse is transferred to the side peaks when the pulse passes through a CFG. Thus the amplitude of the side peaks grows linearly with the number of CFGs along the transmission distance, which makes such systems very prone to ISI [7]. In a previous work, we have shown that the use of DM solitons, unlike in linear systems, inhibits the growth of side peaks induced by GDR [3]. In other words, the use of DM solitons permits to maintain the

<sup>3</sup> Present address: Department of Engineering, Fraser Noble Building, King's College, University of Aberdeen, Aberdeen AB24 3UE, UK.

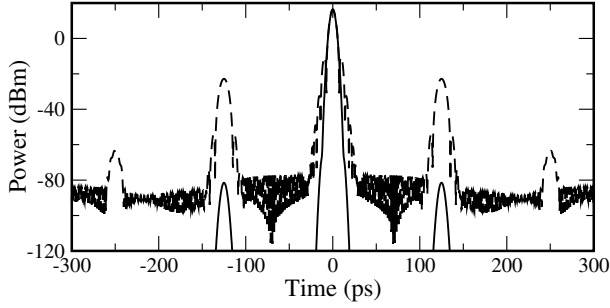


**Figure 1.** Temporal pulse shapes having the same energy and width in the lossless DM system without NOLMs (dashed) and with NOLMs (solid). The GDR is modelled by a sinusoidal function.

amplitude of the side peaks within a level which is relatively small but non-zero. Consequently in DM communication systems compensated by CFGs, there always exists residual side peaks which may also induce a certain amount of ISI. On the other hand, it has been demonstrated that nonlinear optical loop mirrors (NOLMs) can be utilized for 2R regeneration in a DM fibre system compensated by dispersion compensating fibres [8–10].

In the present work, we show that an appropriate combination of the DM soliton and NOLM actions permits a dramatic reduction of the side peaks induced by GDR in grating-compensated DM soliton systems. The DM soliton acts by setting a strict limit in the growth of the side peaks induced by the GDR. The residual side peaks which have survived the soliton action are then reduced substantially by the NOLMs. We show that, with this method, one can improve the transmission distance by more than one order of magnitude when compared with a system without NOLMs. The possibility of reducing the side peaks by the use of NOLMs was recently suggested in lossless grating-compensated DM soliton systems [11], and in lossy DM soliton systems [12]. But in these studies, an evaluation of the transmission performances of the systems with and without NOLMs has been made by adopting different input conditions (pulse energy and width) for the two types of systems (system without and with NOLMs). To obtain a rigorous evaluation of the effectiveness of the proposed method, we have carried out in the present work a comparison of the transmission performances of the two types of systems, for the same input conditions. To this end, we have shown that in DM soliton systems with and without NOLMs there exist DM soliton solutions having the same energy and width. Using those DM solitons we have carried out a rigorous comparison between the transmission performances of the two types of systems. In particular we have found that the transmission distance can be improved by more than one order of magnitude in the system with in-line NOLMs when the two first (or major) side peaks of each pulse are located exactly at the centre of two adjacent bit slots, which is a situation for maximum ISI [13]. We have also studied the NOLM action in different conditions of ripple periods and ripple amplitudes, and found that propagation can achieve transoceanic distances for a ripple period as long as 24 GHz at a ripple amplitude of 5 ps, and for a ripple amplitude as large as 20 ps at a ripple period of 8 GHz.

This paper is organized as follows. In section 2 we present the system modelling and related equations. Then, we compare the soliton solutions in the system without and with NOLMs in lossless and lossy grating-compensated DM soliton systems in sections 3 and 4, respectively. Finally, we conclude in section 5.

## 2. System modelling

Pulse propagation in an optical fibre system with periodically varying dispersion and Kerr non-linearity is governed by the nonlinear Schrödinger (NLS) equation

$$i \frac{\partial q}{\partial z} - \frac{\beta(z)}{2} \frac{\partial^2 q}{\partial t^2} + \gamma |q|^2 q = 0, \quad (1)$$

where  $q$  is the slowly varying envelope of the electrical field, and  $\beta(z)$  and  $\gamma$  represent the group velocity dispersion (GVD) and self-phase modulation parameters, respectively. Here we have neglected the third-order dispersion and higher-order nonlinear effect because the pulse width considered in this work is greater than 5 ps. The GVD parameter  $\beta(z) = \beta$  for  $z \neq (n + 1/2)L$ , where  $L$  is the length of dispersion map and  $n$  is an integer. The gratings are located at  $z = (n + 1/2)L$  and their actions are given by the transfer function  $F(\omega)$  such that  $Q_{\text{out}}(z, \omega) = F(\omega)Q_{\text{in}}(z, \omega)$ , where  $\omega$  is the angular frequency, and  $Q_{\text{in}}$  and  $Q_{\text{out}}$  are the pulse spectra before and after the gratings, respectively.

In real CFGs, the structure of the GDR is rather complex and depends on the CFG parameters such as the apodization profile [6, 14], the grating length, etc. For simplicity, one can consider a sinusoidal form of ripples, and assume that the grating reflectivity bandwidth is much greater than the signal bandwidth [3]. Then the transfer function becomes

$$F(\omega) = \exp \left[ i \frac{g}{2} \omega^2 - i \frac{\Gamma}{T_0} \cos(\omega T_0 + \theta) + i \frac{\Gamma}{T_0^2} \right], \quad (2)$$

where  $g$  is the average lumped dispersion of the grating. The average dispersion of the system is  $\bar{\beta} = (\beta L + g)/L$ . The parameters  $\Gamma$ ,  $2\pi/T_0$ , and  $\theta$  are the amplitude, period, and phase of the grating dispersion ripples, respectively. The parameter  $T_0$  is the temporal separation between the side peaks induced by the GDR. The lumped dispersion of the grating is therefore given by  $g + \Gamma \cos(\omega T_0 + \theta)$ .

To be more realistic, one can also obtain the grating transfer function  $F(\omega)$  by solving a set of coupled-mode equations [15], which include all the major parameters of the grating, namely, the length of the gratings and the apodization profile. The equations coupling the two propagation modes in the CFGs are given by [15]

$$\frac{dR}{dz} - i \left[ \kappa_{\text{dc}} + \frac{1}{2} \left( \Delta\beta - \frac{d\phi(z)}{dz} \right) \right] R = i\kappa_{\text{ac}} S, \quad (3)$$

$$\frac{dS}{dz} + i \left[ \kappa_{\text{dc}} + \frac{1}{2} \left( \Delta\beta - \frac{d\phi(z)}{dz} \right) \right] S = -i\kappa_{\text{ac}}^* R, \quad (4)$$

where  $R$  and  $S$  are, respectively, the forward and backward propagation modes,  $\kappa_{\text{dc}}$  is the dc coupling constant which is a function of the average refractive index of the grating, and  $\kappa_{\text{ac}}$  is the ac coupling constant, which is a function of the amplitude

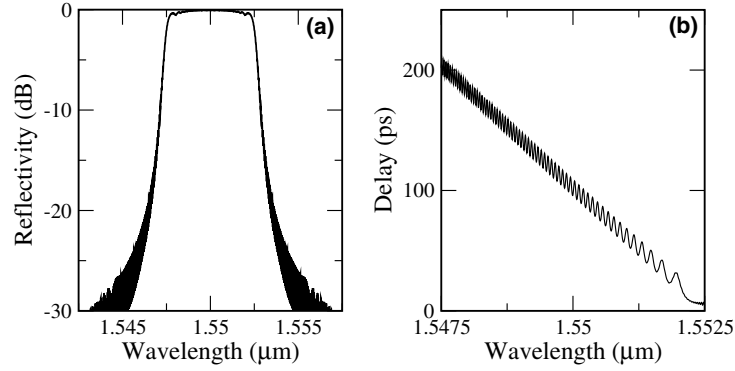


**Figure 2.** (a) Reflectivity and (b) group delay spectra of the grating that is obtained by solving the coupled-mode equations.

of the refractive index variation of the grating. The parameter  $\Delta\beta$  is the difference between the propagation constant of the forward and backward propagating modes,  $\phi(z)$  is the phase change within the grating, and the symbol \* represents the complex conjugate.

### 3. Lossless DM soliton systems using CFGs

It has been reported that soliton solutions exist in grating-compensated DM fibre systems with GDR in the gratings [3]. On the other hand, an evaluation of the suppression of the side peaks in lossless systems with and without NOLMs has been done in [11], but with different input conditions, which does not provide a fair comparison between these two types of systems. Here, we compare the dynamical behaviours of soliton solutions having both the same pulse energy and width in lossless DM soliton systems with and without NOLMs, compensated by CFG with GDR. The DM soliton solutions are obtained by numerically solving the NLS equation (1), with use of the transfer function  $F(\omega)$ . We consider two types of grating modelling. First, the GDR is modelled by the sinusoidal function, equation (2). Second, the grating profile is obtained by solving the coupled-mode equations (3) and (4).

We consider a system which consists of 40 km of fibre segment with a CFG inserted at the middle of the fibre segment. The dispersion and nonlinearity of fibres are  $1.06 \text{ ps nm}^{-1} \text{ km}^{-1}$  and  $2 \text{ km}^{-1} \text{ W}^{-1}$ , respectively. The average lumped dispersion of the gratings is  $-39.2 \text{ ps nm}^{-1}$  with ripple amplitude of 5 ps and period of 0.064 nm (8 GHz) [7] for the sinusoidal ripples. For coupled-mode equations, the CFG has a length of 2 cm, and we adopt a Gaussian apodization function [14]. In this function, the amplitude of the refractive index variation along the grating is

$$\kappa_{ac}(z) = \Delta n_{\text{eff}} \exp \left[ \frac{-2(z - 0.5L_g)^2}{L_g^2} \right],$$

where  $\Delta n_{\text{eff}}$  is the amplitude of the index fluctuation and  $L_g$  is the grating length. We choose the maximum index fluctuation to be  $1.2 \text{ mm}^{-1}$  and the dc coupling constant  $\kappa_{dc} = 0$ . The phase change ( $d\phi/dz$ ) is equal to  $C(z - 0.5L_g)/L_g^2$  and  $C \sim 845$ . The grating reflectivity and delay spectra are shown in figures 2(a) and (b), respectively. Thus the average dispersion of the system is  $0.08 \text{ ps nm}^{-1} \text{ km}^{-1}$ . We place an amplifier with gain of 12 dB just before each NOLM to increase

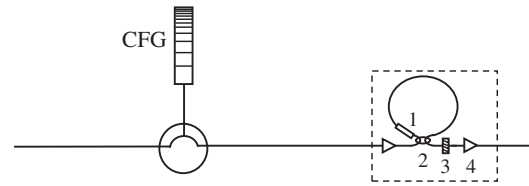


**Figure 3.** Schematic of one span of the lossless transmission system. The dashed box shows the configuration of the NOLM, which includes the following elements: 1: attenuator; 2: 50:50 coupler; 3: filter; 4: amplifier.

the pulse nonlinearity so that it can reduce the loop length. A period of the transmission system is schematically represented in figure 3. In the NOLM, we choose the splitting ratio of 0.5 and use a loss element to break the symmetry between the two waves emerging from the splitter, and add an amplifier after the loop to balance the loss in the loop. The loss and gain, in the attenuator and amplifier (after the loop), are 8.47 and 1.82 dB, respectively. We assumed that the NOLM is constructed from a dispersion-shifted fibre. The loop length is  $\sim 2.96 \text{ km}$ , and the cross-section area is considered to be  $25 \mu\text{m}^2$ . A Gaussian-shaped filter with full width at half maximum bandwidth of 110.3 GHz is placed after the loop to re-shape the output pulse.

In the system without NOLMs, the stationary solution is obtained using the numerical averaging method developed by Nijhof *et al* [16]. We launch the Gaussian pulse with energy of 0.22 pJ and width of 5 ps into the systems with NOLMs and the propagating pulse converges itself to a stationary solution. Using the sinusoidal form for the ripples in CFGs we obtain the temporal profiles of the stationary solitons having essentially the same energy and same width in the systems without (dashed) and with (solid) NOLMs, as figure 1 shows. Thus, for the two systems, we obtain different stationary profiles having almost the same energy of 0.22 pJ and the same width of  $\sim 4.8 \text{ ps}$  (4.9 and 4.7 ps in the systems without and with NOLMs, respectively). Here the pulse profile is taken right after each NOLM, whereas for the system without NOLMs we consider the pulse profile at the middle of each fibre segment (of 40 km). The soliton solution has many satellite peaks and the separation between any two peaks is 125 ps. This 125 ps separation is fixed by the ripple period (8 GHz) which we have considered for the GDR. The side peak separation is inversely proportional to the ripple period. The peak power of the main

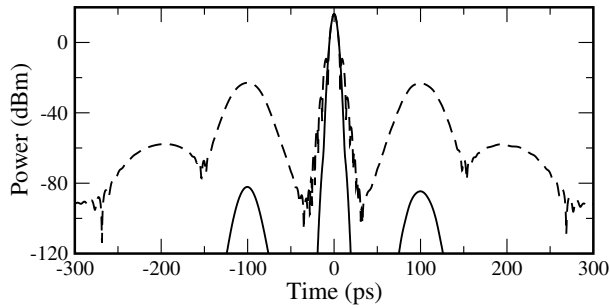


**Figure 4.** Temporal pulse shapes having the same energy and width in the lossless DM system without NOLMs (dashed) and with NOLMs (solid). The grating is modelled by the coupled-mode equations.

peak in both systems are nearly the same: 16 dBm. The most outstanding result in figure 1 is that the peak powers of the first side peaks (the two nearest neighbours of the central peak) settle to  $-22.8$  and  $-81.5$  dBm, in the system without and with NOLMs, respectively. Thus, the NOLM action leads to a reduction of the power of the major side peaks induced by GDR by  $\sim 59$  dBm.

For the grating modelled by the coupled-mode equations, the temporal soliton profiles having the same energy, 0.21 pJ, in the systems with and without NOLMs are represented in figure 4. The pulse widths are found to be 4.8 and 4.6 ps in the systems without and with NOLMs, respectively. In the system without NOLMs, an amplifier of 0.064 dB gain is placed at the middle of fibre segments to compensate for the power loss in the grating reflectivity profile. The gain is equivalent to the reflectivity of the grating at  $1.55 \mu\text{m}$ . The shape of the DM soliton solutions is asymmetric since the structure of the GDR is not symmetric while modelled by the coupled-mode equations. The first side peaks are located at 99.8 ps (in the system without NOLMs) and 100 ps (in the system with NOLMs), which provides an effective ripple period from CFGs of about 10 GHz. On the other hand, here also, where we use a model of coupled-mode equations for the grating, there exists an asymmetry in the side peaks powers, but which is only slightly visible in figure 4. Without NOLMs, the peak power of the left first side peak is  $-22.9$  dBm and the right side peak is  $-23.2$  dBm calculated just after the amplifiers. For the system with NOLMs, the first side peaks have peak powers of  $-82.1$  dBm (left) and  $-84.6$  dBm (right) after the NOLMs. The power of the main peak in both systems is nearly the same: 16 dBm. But the most important result in figure 4 is that the powers of the first side peaks of the soliton solution in the DM fibre system with NOLMs are reduced by about  $\sim 59$  dB when compared to the system without NOLMs.

The results show that the peak power associated with the side peaks of the DM solitons in CFG-compensated DM fibre systems can have a substantial reduction of around 59 dB, by introducing a NOLM in every dispersion map in both the case of sinusoidal GDR and using the coupled-mode equations to model the CFGs.

#### 4. Lossy DM soliton systems using CFGs

For practical usage, it is important to investigate the effectiveness of NOLMs in grating-compensated DM fibre

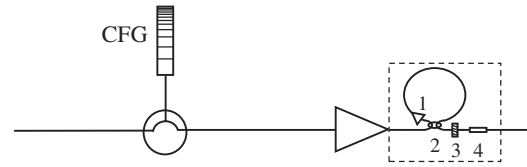


**Figure 5.** Schematic of one amplification span of the lossy transmission system; the dashed box shows the configuration of the NOLMs. 1: amplifier; 2: 50:50 coupler; 3: filter; 4: attenuator. The amplifier is located at the end of the span.

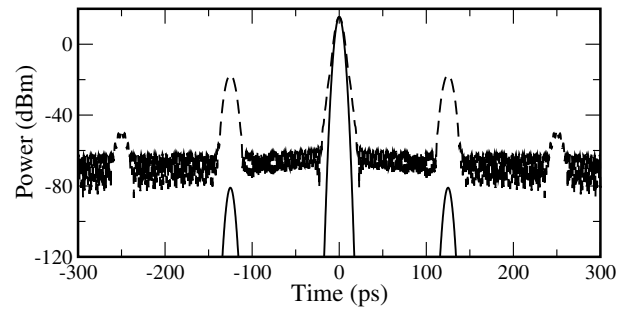


**Figure 6.** Temporal pulse shapes having the same energy and same width in the lossy DM systems without NOLMs (dashed) and with NOLMs (solid). The GDR is modelled by a sinusoidal function.

systems with fibre loss and periodic amplification. It has been suggested that the effects of GDR can be reduced in lossy DM fibre systems with the help of NOLMs [12]. But the operating conditions used in [12] do not permit a rigorous evaluation of the performance gain induced by the NOLMs. Here, we modify the configuration of the NOLMs so as to make use of soliton solutions that possess the same energy and width as in the system without NOLMs. Then we carry out a clear and rigorous evaluation of the transmission performances of the systems with and without NOLMs.

We consider the same dispersion map as that of the lossless DM fibre systems and include a fibre loss coefficient of  $0.2 \text{ dB km}^{-1}$ . The GDR is the same as that in lossless systems. The amplifiers are placed at the middle of fibre segment [17] and followed by NOLMs. Thus the amplifier and NOLM spacings are the same as the length of dispersion map, i.e., 40 km. The configuration of one amplification span of the system is schematically represented in figure 5. The amplifiers in the transmission line have a gain of 8 dB (without NOLMs) or 8.78 dB (with NOLMs). The extra gain in the system with NOLMs is needed to compensate the total power loss in the NOLMs. In lossy systems, we replace the attenuator in the loop by an amplifier with a gain of 17 dB in order to reduce the loop length to 1 km. We include the loss coefficient of  $0.3 \text{ dB km}^{-1}$  in the loop and add a filter (bandwidth of 110.3 GHz) to reshape the pulse. The loss element after the filter is to balance the extra gain in NOLMs, and its value is  $-13.19$  dB.

The stationary solutions are determined numerically by applying the averaging method [16] in the lossy DM soliton systems without the NOLMs. For the system with NOLMs, we gradually adjust the gain of the amplifiers in the transmission line until the gain converges to a stable value [18], which corresponds to a stationary solution. Figure 6 shows the stationary profile measured just after the amplifier, by using

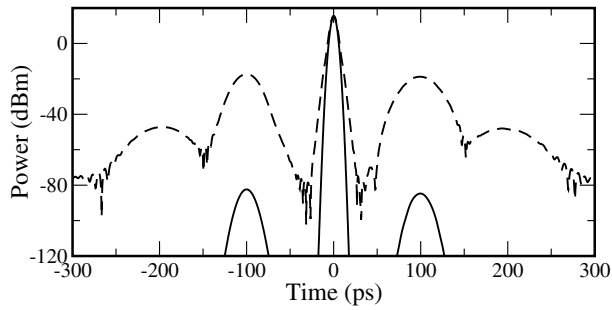


**Figure 7.** Temporal pulse shapes having the same energy and nearly same width in the lossy DM system without NOLMs (dashed) and with NOLMs (solid). The grating is modelled by the coupled-mode equations.

a sinusoidal model of GDR, in the systems without (dashed curve) and with (solid curve) NOLMs. The sinusoidal GDR has an amplitude of 5 ps, period of 0.064 nm (8 GHz), and the relative phase of  $\pi$ . The pulse energy just after the amplifiers is the same, 0.224 pJ, and the width is nearly the same: 5.95 ps for system without NOLMs and 5.09 ps for system with NOLMs. The decrease of the pulse width is due to the extra nonlinearity introduced by the NOLMs. The side peak suppression is 64 dB. We also use the grating profile modelled by the coupled-mode equations in figure 2 to obtain the stable solutions in the systems, and the pulse shapes are shown in figure 7. The pulse energy is same as in the case of sinusoidal ripples. The pulse widths are 5.71 ps (without NOLMs) and 5.06 ps (with NOLMs) in the systems. In this case, we find the first side peaks locations in the system without and with NOLMs are 100 ps and the side peak suppression is about 65 dB.

To examine the transmission performance of the systems without and with NOLMs, we launch the stable solution as a bit pattern [011110101100100] into the systems. The bit slot is chosen to be equal to the separation between the central peak and the side peaks, that is 125 ps, so that the central peak of each pulse exactly overlaps with the first side peaks of the adjacent pulses, which corresponds to a situation of maximum ISI [13]. Figure 8 shows the  $Q$ -factors along the propagation distance without (dashed curve) and with (solid curve) NOLMs in the system using gratings with sinusoidal ripples. The value  $Q = 6$  (dotted line) corresponds to a bit-error rate of  $10^{-9}$ . The error-free transmission distances without and with NOLMs are 0.36 Mm and  $> 10$  Mm, respectively. In the system with NOLMs, the  $Q$ -factor fluctuates transiently and becomes stable as the propagation distance increases. The peak power of the pulses is stabilized by the NOLMs [10, 19]. We find that the bit sequence has error-free transmission even up to 20 Mm. The corresponding eye diagrams of the system without and with NOLMs are shown in figures 9(a) and (b), respectively. The power fluctuation in the system without NOLMs, as shown in figure 9(a), is caused by the energy exchange between the central peak and the side peaks of the pulse. As the use of NOLMs in the DM fibre system significantly suppresses the side peaks, the energy exchange between the central peak and the side peaks, and the resulting amplitude jitter, are dramatically reduced (see figure 9(b)).

In the context of bit cost reduction, an important question that could be raised is whether the above-mentioned

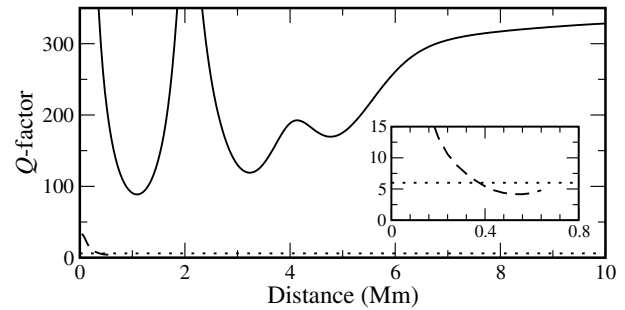


**Figure 8.** The  $Q$ -factors versus propagation distance in the lossy grating-compensated DM systems without NOLMs (dashed) and with NOLMs (solid). The GDR is modelled by a sinusoidal function with amplitude of 5 ps and period of 8 GHz. The size of the bit window is equal to the separation of side peaks, 125 ps.

performances (of systems using NOLMs) are preserved if the NOLM spacing is increased. To gain some insight into this question, we have carried out numerical simulations in which the NOLM spacing is fixed to four times the amplifier spacing, i.e., 160 km. As it is obvious that any increase of the NOLM spacing inevitably causes the amplitude jitter to increase, a more careful and refined optimization of the NOLM is required to limit the growth of this jitter. To this end, we have slightly modified the system design in a way such that the amplifier lying before each NOLM has a gain of  $\sim 7.47$  dB and the gain of the amplifier in the loop is increased to 17.7 dB. The pulse width was set to 5.5 ps, which is less than the pulse width for the system having a NOLM at every amplifier site. The system, pulse and the ripple parameters have been kept to be the same values as in the case of figure 6 where the NOLM spacing coincides with the amplification spacing. A careful inspection of figure 10, which shows the stationary solution measured just after the NOLMs, reveals that the amount of energy transfers from the main to the side peaks is increased (when compared with the case of figure 7). This is due to a larger number of CFGs between two consecutive NOLMs. Also, as the number of CFGs between the NOLMs is increased, the side peak suppression (the difference between the cases with and without NOLMs) is reduced to 46 dB. The  $Q$ -factors along the propagation distance, which we have evaluated after every amplifier in the system without (dashed curve) and with (solid curve) NOLMs, are shown in figure 11. The  $Q$ -factor (for the system with NOLMs) exhibits an oscillating behaviour, having maximum values after the amplifier sites that contain a NOLM. But the most important point that emerges from figure 11 is that error-free transoceanic transmissions could also be achieved when the NOLM spacing is equal to four times the amplifier spacing. Thus, it is quite possible to design DM soliton systems compensated by CFGs using NOLMs, with relatively large NOLM spacing, without excessively sacrificing the transmission performances. As the problem of the optimum location of the NOLMs in the transmission system is beyond the scope of the present study, in what follows, we will focus on the basic system in which the amplifier spacing coincides with the NOLM spacing.

We have also launched the bit pattern into the systems with the actual grating parameters as shown in figure 2. Since the side peak separation is 100 ps, it represents the effective ripple

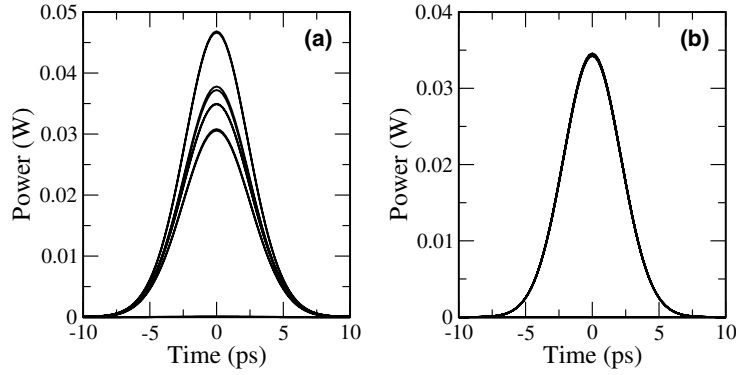


**Figure 9.** The eye diagram in the system (a) without and (b) with NOLMs at 0.36 and 10 Mm, respectively.

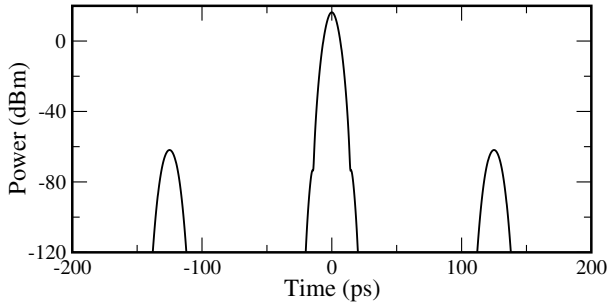


**Figure 10.** Temporal pulse shape in the lossy DM systems with a NOLM implemented after every four amplifiers. The system and GDR parameters are the same as in figure 6.

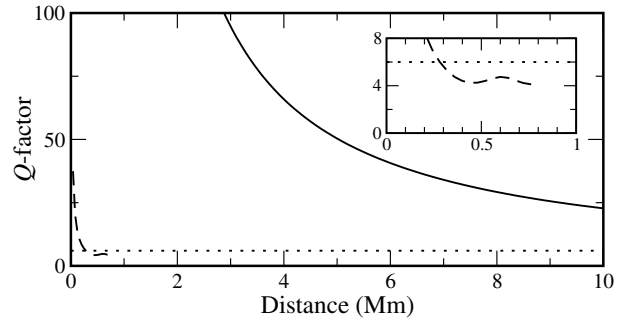


**Figure 12.** The  $Q$ -factors versus propagation distance in the lossy grating-compensated DM systems without NOLMs (dashed) and with NOLMs (solid). The grating is modelled by the coupled-mode equations. The size of the bit window is equal to the separation of side peaks, 100 ps.

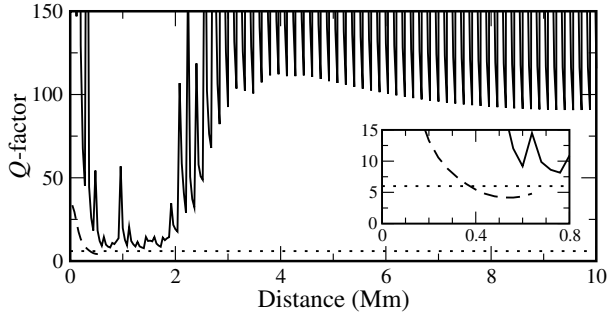


**Figure 11.** The  $Q$ -factors versus propagation distance in the lossy grating-compensated DM systems without NOLMs (dashed) and with NOLMs (solid). The NOLM spacing is four times the amplifier spacing. The system and GDR parameters are the same as in figure 8.

period of 10 GHz which is larger than that in the sinusoidal ripples (8 GHz). Thus we choose the pulse separation of 100 ps such that the main peak of each pulse is exactly located on the side peaks of the adjacent pulses. The  $Q$ -factors of the pulses along the transmission distance without (dashed and inset) and with (solid) NOLMs are shown in figure 12. The transmission distance in the system with NOLMs (10 Mm) is 30 times longer than that without NOLMs (0.28 Mm). Figures 13(a) and (b) illustrate the eye diagrams of the system without and with NOLMs. We find that the timing jitter is prominent over the amplitude jitter after 1 Mm in the system with NOLMs and it is caused by the asymmetric delay spectrum of the actual grating profile as shown in figure 2(b). The timing  $Q$ -factor

is calculated using the definition  $Q_T \equiv 0.7T_b/\sigma_t$ , where  $T_b$  is the size of bit slot and  $\sigma_t$  is the standard deviation of the bit '1' with respect to the centre of the bit slot. The timing  $Q$ -factor in figure 12 is calculated with a bit slot of 100 ps. For a pulse width of 5 ps, the timing jitter is typically calculated by choosing  $T_b$  as 25 ps, and we find that the  $Q$ -factor drops to 6 at 9.52 Mm in this simulation. At the locations just after CFGs, the power of the left and right first side peaks is respectively  $-21.6$  and  $-27$  dBm. These unbalanced side peak powers induce timing jitter.

Thus, the above results show that the combined use of the DM solitons and NOLMs can effectively improve the system performance and permit transoceanic transmissions in the presence of GDR, irrespective of whether the GDR is modelled by a sinusoidal function or the coupled-mode equations in lossy CFG-compensated DM fibre systems.

#### 4.1. Tolerance with respect to variations in the GDR

In previous sections, we have shown that the use of NOLMs can improve the system performance in grating-compensated DM soliton systems. In this subsection, we investigate the tolerance of the system performance with respect to variations in the GDR parameters, in the transoceanic transmissions in the same system as that shown in figure 5. From equation (2) one can see that the effect of ripple in the phase of the transfer function  $F(\omega)$  is proportional to the group delay ripple

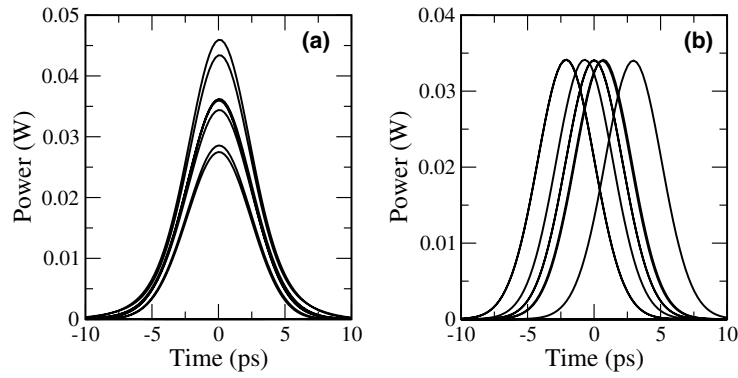


**Figure 13.** The eye diagram in the lossy system (a) without and (b) with NOLMs at 0.28 and 10 Mm, respectively.

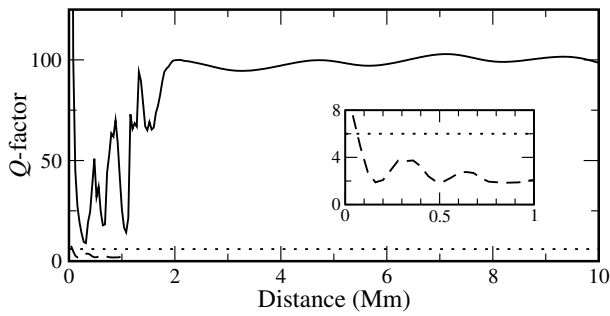


**Figure 14.** The  $Q$ -factors versus propagation distance in the lossy systems without NOLMs (dashed and inset) and with NOLMs (solid). The GDR is modelled by a sinusoidal function with amplitude of 20 ps and period of 8 GHz.

amplitude ( $\Gamma/T_0$ ) and ripple period ( $2\pi/T_0$ ). This means that the effect of GDR should be large if the group delay ripple amplitude or the ripple period is large. In [3], we have shown that the increment of the ripple period will result in a large contribution of GDR to the effective grating dispersion when the signal bandwidth is unchanged.

To study the tolerance of the systems with respect to the variations in the GDR, it is easier to model the GDR by the sinusoidal function rather than by the coupled-mode equations because the parameters in the coupled-mode equations have no direct relationship with the parameters of the GDR. We thus choose the sinusoidal function to

model the GDR parameter variation and launch a periodic 32-bit pattern [10010011011101000110010010100111] of stationary solutions in the systems. We find that the use of NOLMs permits us to achieve transoceanic transmissions for a ripple amplitude as high as 20 ps for a fixed ripple period of 8 GHz. Figure 14 shows the  $Q$ -factors without (dashed) and with (solid) NOLMs in the systems. Thus, the inset which shows the  $Q$ -factor of the system without NOLMs, exhibits fluctuations in the  $Q$ -factor, which we attribute to the energy exchange between the central peak and the side peaks. Here, the maximum distance of transmission is increased by more than 100 times when using NOLMs. The corresponding eye diagram in the system with NOLMs at 10 Mm is shown in figure 15(a). We also study the extreme case scenario where all 32 bits are '1'. We find that the phase of the first side peaks (left and right) of the stationary solutions is the same. Thus the side peaks cannot be cancelled by the phase difference in consecutive '1's as in the linear systems [7]. In the DM fibre system with NOLMs, we find that the error-free distance settles to 2.6 Mm when the ripple amplitude is 20 ps and goes up to 10 Mm when the amplitude is 10 ps for a fixed ripple period value of 8 GHz.

Next, the GDR amplitude is kept constant at 5 ps and we increase the value of the ripple period. As the ripple period increases, the separation between the central peak and the side peaks reduces. For the maximum ISI situation, we choose the bit slot to be same as the side peak separation. Thus the transmission rate will be equal to the ripple period. In this

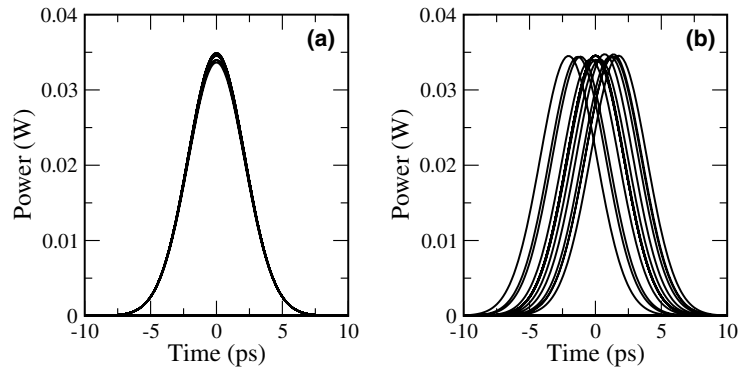


**Figure 15.** The eye diagram in the lossy system with NOLMs at 10 Mm. The GDR has an amplitude of (a) 20 ps and (b) 5 ps, and a period of (a) 8 GHz and (b) 24 GHz.

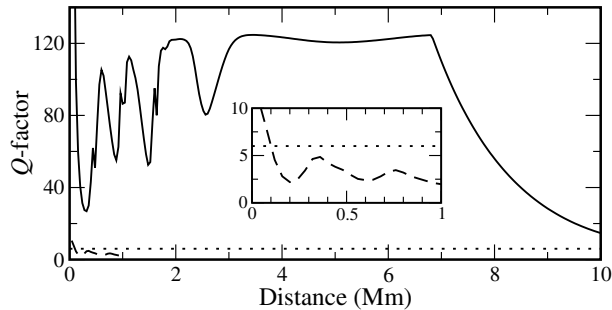


**Figure 16.** The  $Q$ -factors versus propagation distance in the lossy systems without NOLMs (dashed and inset) and with NOLMs (solid). The GDR amplitude is 5 ps and the period is 24 GHz.

situation we have found that the transoceanic transmission is achieved when the ripple period is as large as 24 GHz at a speed of 24 Gb/s. The  $Q$ -factors are shown in figure 16 for the DM fibre systems without (dashed) and with NOLMs (solid). Figure 15(b) illustrates the eye diagram for the system with NOLMs at 10 Mm.

We find that the performance of the transmission line is limited by the ripple period and not by the map configuration itself. That is, for the same DM fibre system, the transmission performance for bit rates higher than 24 Gb/s is possible in the absence of GDR. In order to study the pulse-to-pulse interaction caused by the map configuration, we consider the same DM fibre system with neither NOLMs nor GDR in gratings (i.e., ideal CFGs). We launch the 32-bit pattern at a higher speed, 32 Gb/s, and a narrower pulse separation, 31.25 ps, and we obtain an error-free transmission over 10 Mm in the system with neither NOLMs nor GDR in CFGs. This shows that the pulse-to-pulse interaction from the dispersion map configuration is not a factor to limit the transmission distance. Also, the drop of the  $Q$ -factor (solid) after 7 Mm in figure 16 is mainly due to the timing jitter caused by the GDR in gratings. Figure 17 shows the pulse shape at the output of the gratings. The solid and dashed curves are respectively the soliton solution in the system with NOLMs and GDR, and with neither NOLMs nor GDR. The side peaks induced by GDR with peak separation of 41.67 ps broadens the tails of the pulse and lead to the timing jitter in figure 15(b). For the extreme case scenario of the bit pattern (all '1's), the transmission can reach distances larger than 10 Mm for a ripple period of 16 GHz and amplitude of 5 ps. These results show that the use of NOLMs allows for a large tolerance with respect to the variations in the GDR of CFGs.

## 5. Conclusions

We have shown that the energy associated with the side peaks of the DM solitons in CFG-compensated DM fibre systems can be considerably reduced by inserting a NOLM in every dispersion map of lossless and lossy systems. The system performance is substantially improved through a reduction of the ISI caused by the side peaks. In the lossy system, we have obtained transoceanic transmission using NOLMs, when the maximum ripple amplitude is 20 ps at a ripple period of 8 GHz and the largest ripple period of 24 GHz for the ripple amplitude of 5 ps. We have shown that the use of NOLMs permits us to

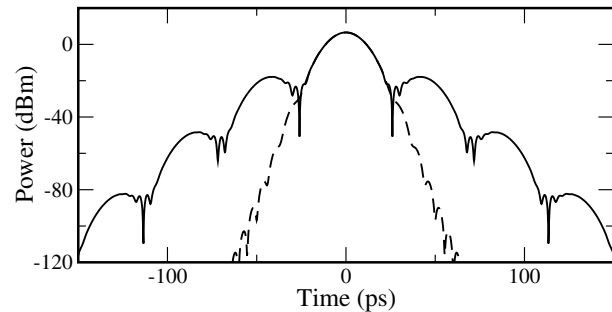


**Figure 17.** Temporal pulse shapes in the lossy DM system without NOLMs or GDR (dashed), and with NOLMs and GDR (solid). The GDR period is 24 GHz.

preserve the transmission performances over large ranges of the GDR parameters. We have also shown that the cost of the implementation of the NOLMs could be reduced by increasing the NOLM spacing.

## Acknowledgments

This work was partially supported by the Research Grant Council of the Hong Kong Special Administrative Region, China, under Project PolyU5242/03E. P Tchofo Dinda acknowledges The Hong Kong Polytechnic University for hospitality.

## References

- [1] Ibsen M and Feced R 2003 Fiber Bragg gratings for pure dispersion-slope compensation *Opt. Lett.* **28** 980–2
- [2] Kumar S and Hasegawa A 1997 Quasi-soliton propagation in dispersion-managed optical fibers *Opt. Lett.* **22** 372–4
- [3] Kwan Y H C, Wai P K A and Tam H Y 2001 Effect of group-delay ripples on dispersion-managed soliton communication systems with chirped fiber gratings *Opt. Lett.* **26** 959–61
- [4] Ania-Castañón J D, García-Fernández P and Soto-Crespo J M 2001 Fiber Bragg grating dispersion-managed multisolitons *J. Opt. Soc. Am. B* **18** 1252–9
- [5] Yamada E, Imai T, Komukai T and Nakazawa M 1999 10 Gbit/s soliton transmission over 2900 km using 1.3  $\mu\text{m}$  singlemode fibres and dispersion compensation using chirped fibre Bragg gratings *Electron. Lett.* **35** 728–9
- [6] Floreani F, Gilooley A, Zhang L, Bennion I, Shu X and Sugden K 2003 A simple method for the fabrication of intrinsically apodized chirped fibre Bragg gratings *J. Opt. A: Pure Appl. Opt.* **5** S59–62
- [7] Evangelides S G, Bergano N S and Davidson C R 1999 Intersymbol interference induced by delay ripple in fiber Bragg gratings *OFC'1999* vol 4, pp 5–7
- [8] Boscolo S, Turitsyn S K and Blow K J 2003 All-optical passive 2R regeneration for  $N \times 40$  Gbit/s WDM transmission using NOLM and novel filtering technique *Opt. Commun.* **217** 227–32
- [9] Seguinéau F, Lavigne B, Rouvillain D, Brindel P, Pierre L and Leclerc O 2004 Experiment demonstration of simple NOLM-based 2R regenerator for 42.66 Gbit/s WDM long-haul transmissions *OFC'2004* vol 1 (Paper WN4)
- [10] Gray A, Huang Z, Lee Y W A, Khrushchev I Y and Bennion I 2004 Experimental observation of autosoliton propagation in a dispersion-managed system guided by nonlinear optical loop mirrors *Opt. Lett.* **29** 926–8

- [11] Kwan Y H C, Nakkeeran K and Wai P K A 2003 Reduction of intersymbol interference in dispersion-managed soliton systems compensated by chirped fiber gratings *The Pacific Rim Conf. on Lasers and Electro-Optics (CLEO/PR'2003)* vol 1, p 130 (Paper W1F-(5)-3)
- [12] Kwan Y H C, Nakkeeran K and Wai P K A 2004 Transmission improvement in grating-compensated dispersion-managed soliton systems using nonlinear optical loop mirrors *The OptoElectronics and Communications Conf./The Int. Conf. on Optical Internet (OECC/COIN'2004)* pp 178–9 (Paper 13P-33)
- [13] Kwan Y H C, Nakkeeran K, Wai P K A and Tchofo Dinda P 2004 Significant improvement of performance in grating-compensated transmission systems using nonlinear optical loop mirrors *Int. Conf. on Optical Communications and Networks* pp 39–42
- [14] Yang C and Lai Y 2000 Improving the spectral sharpness of an apodized fibre grating *J. Opt. A: Pure Appl. Opt.* **2** 422–5
- [15] Kashyap R 1999 *Fiber Bragg gratings* (San Diego, CA: Academic) chapter 4
- [16] Nijhof J H B, Forsysak W and Doran N J 2000 The averaging method for finding exactly periodic dispersion-managed solitons *IEEE J. Sel. Top. Quantum Electron.* **6** 330–6
- [17] Kutz J N and Wai P K A 1998 Ideal amplifier spacing for reduction of Gordon-Haus jitters in dispersion-managed soliton communications *Electron. Lett.* **34** 522–3
- [18] Boscolo S, Nijhof J H B and Turitsyn S K 2000 Autosoliton transmission in dispersion-managed systems guided by in-line nonlinear optical loop mirrors *Opt. Lett.* **25** 1240–2
- [19] Smith N J and Doran N J 1995 Picosecond soliton transmission using concatenated nonlinear optical loop-mirror intensity filters *J. Opt. Soc. Am. B* **12** 1117–25